BBAA VI International Colloquium on:
Bluff Bodies Aerodynamics & Applications
Milano, Italy, July, 20-24 2008

AERODYNAMIC CHARACTERISTICS OF SPLIT DECK SECTIONS FOR LONG SUSPENSION BRIDGES

Elena Dragomirescu[*], Haeyoung Kim[†], and Tetsuya Kitagawa[*]

[*]EcoTopia Science Institute
Nagoya University, Chikusa, Furocho, 464-8603 Nagoya, Japan
e-mails: elndrag@esi.nagoy-u.ac.jp, kitagawa@civil.nagoya.u-ac.jp

[†] Department of Civil Engineering
Nagoya University, Chikusa, Furocho, 464-8603 Nagoya, Japan
e-mail: kim@civil.nagoya-u.ac.jp

Keywords: Split Deck Sections, Aerodynamic Characteristics, CFD, Wind Flow Simulation.

1 INTRODUCTION

With the increase of span for suspension bridges, new challenges were addressed regarding the aerodynamic shape of the bridge deck. Therefore bridge deck sections have evolved achieving better aerodynamic shapes, as the deck section proposed for super long Messina Suspension Bridge [1]. Nowadays functionality requirements of the bridge involves not only span lengths of 3000 m and more, but also a deck width which can offer space for railways and traffic lanes in the same time, therefore various modifications and splitting of the basic box-girder deck have been analyzed herewith.

One of the new proposals of a split deck shape for suspension bridges, which is expected to achieve very long span lengths, is a box-girder deck as in Fig. 1(a), which consists of two side decks for traffic lanes and two middle decks for railway a total of 3 gaps separating them. Wind flow simulations have been performed on a model reduced to scale 1:30, for Re = 8×10^5 and aerodynamic drag and lift components along with pressure distribution on upper and lower part of each deck have been analyzed. A comparison has been made with the results obtained from a standard split deck, of similar dimensions, tested under same flow conditions.

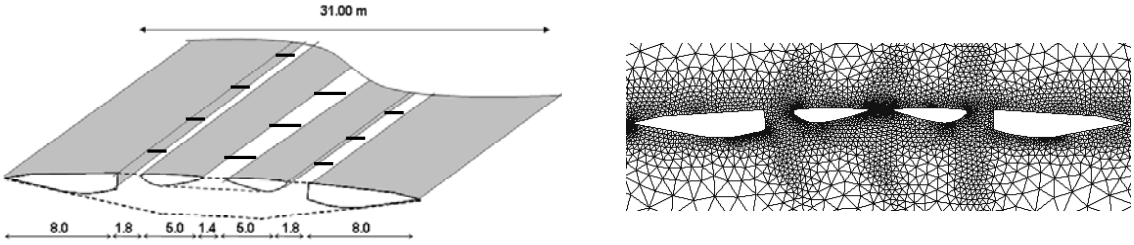

Figure 1: Multiple-gap deck section (a) Geometric dimension (b) Mesh detail.

2 SIMUALTION METHOD

Wind flow around bridge deck sections was simulated by solving the 2D Navier-Stokes equations for unsteady, incompressible flow, by finite volume method (FVM) considering a QUICK upwind scheme for non-linear (convection-diffusion) terms. Pressure and velocities corrections were considered for Poisson pressure equation and UMFPACK was used when solving the sparse matrices, while momentum equations were solved by Runge-Kutta method. Simulations were carried out for a Delaunay triangular unstructured mesh, where no slip boundary conditions for deck surface, in flow initial condition for horizontal velocity and out-flow condition based on extrapolated values of horizontal and vertical velocity components were employed [2].

3 AERODYNAMIC CHARACTERISTICS OF DECK SECTIONS

3.1 Split deck section

For $\alpha = 0°$, the wind flow, will slightly separate from the deck surface and will shed alternate vortices behind the first deck, which will reattach onto the second deck on the inner gap region. After reattachment these will combine with the shear layers above and below the second deck, determining separating bubbles which will travel along the deck surface till the end flange where it will separate from bridge deck and will alternately travel downstream (Fig.2(a)). For the case of $\alpha = -5°$, (Fig.2(b)) on the upper deck, the shear layer will separate from the first deck, near the corner and will not reattach on it. Under deck, the shear layer shed from the first deck will reattach onto the second deck in the gap region and will be redirected on the upper side of the deck; a vortex will be formed and will constantly exist inside the gap. Also on the upper side of second deck wind flow will separate at the first corner and will intermittently reattach on the deck. For $\alpha = 5°$, (Fig. 2(c)), a similar pattern was registered but flow behavior was reversed on upper and lower decks: on the lower deck a detachment from first deck follow by a reattachment on the second deck was noticed, while on the upper deck the streamlines will travel parallel with the deck surface till the gap when it will be redirected to under deck.

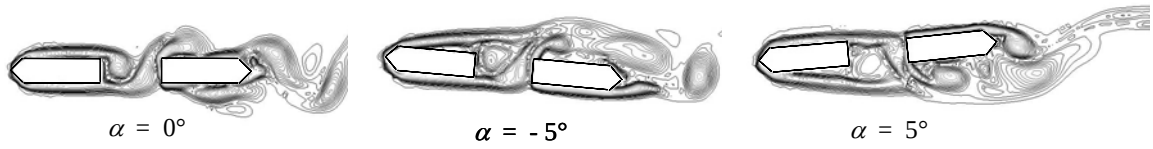

Figure 2: Streamlines around split deck for (a) $\alpha = 0°$, (b) $\alpha = -5°$and (c) $\alpha = 5°$.

Figure 3 represents distribution of mean pressure coefficients on upper decks (Fig. 2(a)) and lower decks (Fig. 3(b)) for various angles of attack: $\alpha = -5°$, 0°, 5°. In general, pressure on both decks was mainly negative indicating a suction which was more accentuated in the separation points. When reattachment took place a sudden increase of pressure was registered, as it will be described bellow. For first deck C_P had a similar distribution in all cases. A negative peak was registered at the corner indicating a wind flow separation from the first deck which can also be noticed in Figs. 3(a), (b) and (c), afterwards stabilizing around $C_Pup = -0.25$. For the second deck, pressure increased till $C_Pup = 0.45$, for the upper deck at $\alpha = 5°$ (Fig.2 (a)) and on lower deck at $\alpha = -5°$ (Fig. 2(b)), indicating a reattachment of the wind flow incoming from the first deck as it can be seen also in Fig. 2(b) and (c). Also it reconfirms the reversed flow patterns for $\alpha = 5°$ and -5°, which was mentioned above. At the far corner of

the deck, a small negative peak is noticed, where wind flow separation takes place. For the rest of the cases, α = 0°, 5° for upper deck (Fig. 2(a)) and α = 0°, – 5° for lower deck (Fig. 2(b)) the *$C_P$down* distribution was smooth and registered values in the range of -0.4 to -0.5.

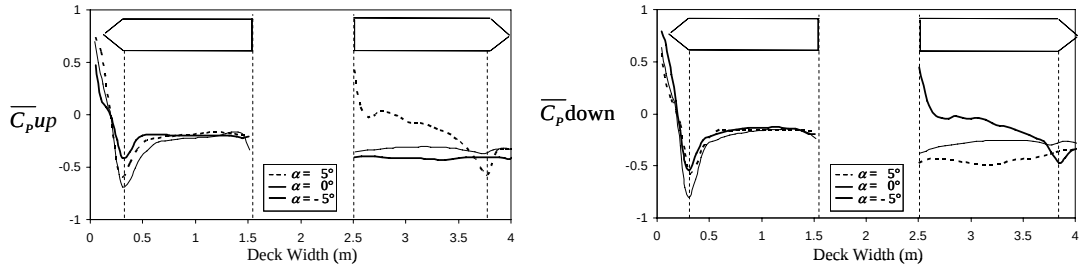

Figure 3: Distribution of mean pressure coefficient for split deck for (a) Upper deck (b) Lower deck.

Aerodynamic lift and drag coefficients will be discussed bellow in comparison with results obtained from multiple – gap deck section.

3.2 Multiple – gap deck section

The wind flow around multiple-gap deck section will become more complicated, slipping through the gaps of the deck and shifting from upper deck to under deck or vice-versa, depending on the angle of attack; also the separation-reattachment phenomena will determine several vortex formations as follows. For α = 0° (Fig. 3(a)), the first 2 decks tend to form a single bluff body and will shed vortices and wind flow will stream around them but it will reattach on the lower surface of 3rd deck. On the upper surface, shear layers separating at the contact with the 3rd deck, in the middle gap region, will form vortices which will travel downward to 4th deck, separating from it in its middle region.

α = 0° α = -5° α = 5°

Figure 4: Streamlines around multiple-gap deck for (a) α = 0°, (b) α = -5°and (c) α = 5°.

For α = -5°, (Fig. 3(b)), the wind flow shed from 1st and 2nd decks will pass through the middle gap and will form vortices, on the upper surface of 3rd deck. Also the shear layers formed under 3rd deck will pass through the last gap and will combine with the shear layer separating from 4th deck resulting in an unstable generation of vortices on the upper surface of the 4th deck. For α = -5°, (Fig. 4(c)), the shear layers incoming from the 1st and 2nd decks, which behave like a single bluff body, will form vortices under deck, in the middle gap area. These, supported by the wind flow coming through the gap from upper surface, will reattach onto the 3rd deck and will be deviated. Finally the vortices shall reattach or just wipe the 4th deck, entirely disconnecting from it in its middle area and traveling downwind.

Distribution of mean pressure coefficient on upper and lower surfaces for all four decks, at α = -5°, 0°, 5° are more unstable than for the case of split deck section. For the first 2 decks, *$C_P$up* has similar distribution for α = 5° and α = 0°, but for 4th deck, *$C_P$up* will become similar for α = 5° and α = -5° (Figs. 5(a)). On the upper side of 3rd deck pressure distribution will be different for each case, *$C_P$up* decreasing with the decrease of α. For all the decks, in the flange area a sudden increase respectively decrease of pressure will be registered, depending on the angle of attack, while for main area of the span *$C_P$up* will take values of -0.1 to 0.1. For

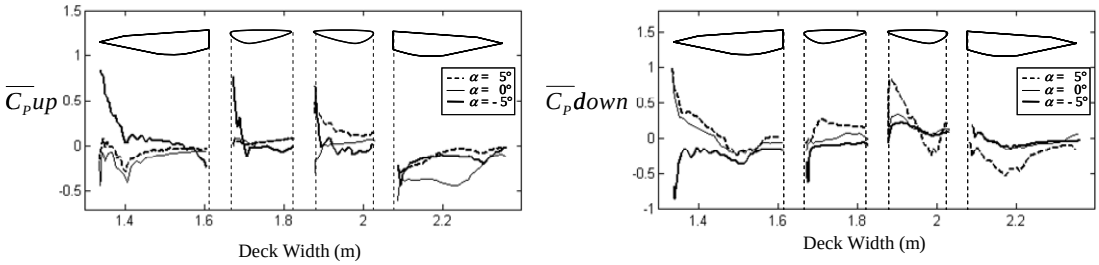

Figure 5: Distribution of mean pressure coefficient for multiple-gap deck for (a) Upper deck (b) Lower deck.

4th deck though, a strong suction will be noticed especially for α = -5° which can be associated with wind flow separation appearing in Figs. 4. The pressure under deck (Fig. 5(b)) will display same evolution for α = 0° and 5° on 1st and 2nd decks and for α = 0° and -5° on 3rd and 4th deck. Also for 3rd deck at α = 5° a change of pressure from 0.9 to -0.3 was noticed indicating a re-attachment of wind flow followed by vortices separation at deck end. For the other decks, in their middle region, $C_P down$ took values between 0.1 and -0.25, depending on α.

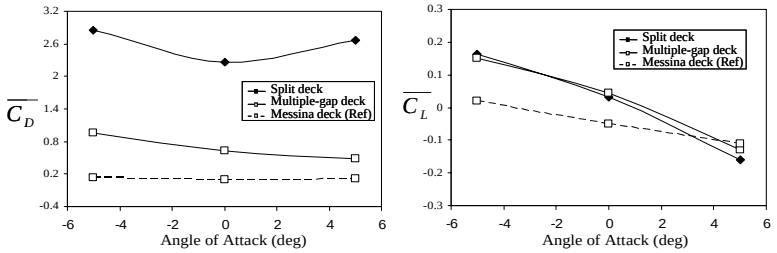

Figure 6: Mean aerodynamic coefficients (a) Drag coefficient, C_D, (b) Lift coefficient, C_L.

Mean drag coefficients determined at α = -5°, 0°, 5°, for split deck was higher than for multiple-gap deck section, while lift coefficients were very similar for the two decks (Figs. 6(a) and (b)). On the other hand, both drag and lift coefficients were higher for multiple-gap deck section than coefficients of Messina deck section, experimentally obtained [1].

4 CONCLUSIONS

Two-dimensional wind flow simulations around split and multiple-gap bridge deck sections have been performed for Re = 8×10^5 at α = -5°, 0°, 5°. The multiple-gap section behaved better in wind flow, lower aerodynamic drag and lift coefficients being obtained. Even if almost in the same range of C_P = 1.0 to -0.8, the pressure distribution was more unstable on both upper and lower decks of multiple-gap deck section, when compared with split deck section. Aerodynamic coefficients reported for Messina deck section [2] were significantly lower. Therefore, detailed wind tunnel experiments shall be performed in order to re-confirm results obtained through the present simulation.

REFERENCES

[1] G. Diana, M. Falco, F. Cheli and A. Cigada. Experience Gained in the Messina Bridge Aerolastic Project. Long Span Bridges and Aerodynamics, Springer, Kobe, Japan, 1999.

[2] S. Kuroda. Numerical Simulation of Flow around Box Girder of a Long Span Suspension Bridge. *Journal of Wind Engineering and Industrial Aerodynamics*, **67-68**, 239–252, 1997.